Quantification of Airway Fibrosis in Asthma by Flow Cytometry

Andrew Reichard[1], **Nicholas Wanner**[1], **Eric Stuehr**[1], **Mario Alemagno**[1], **Kelly Weiss**[1], **Kimberly Queisser**[1], **Serpil Erzurum**[1,3], and **Kewal Asosingh**[1,2]

[1]Department of Pathobiology, Lerner Research Institute, Cleveland Clinic, Cleveland Ohio

[2]Flow Cytometry Core, Lerner Research Institute, Cleveland Clinic, Cleveland Ohio

[3]Respiratory Institute, Cleveland Clinic, Cleveland Ohio. The Cleveland Clinic, Cleveland, Ohio

Abstract

Airway fibrosis is a prominent feature of asthma, contributing to the detrimental consequences of the disease. Fibrosis in the airway is the result of collagen deposition in the reticular lamina layer of the subepithelial tissue. Myofibroblasts are the leading cell type involved with this collagen deposition. Established methods of collagen deposition quantification present various issues, most importantly their inability to quantify current collagen biosynthesis occurring in airway myofibroblasts. Here a novel method to quantify myofibroblast collagen expression in asthmatic lungs is described. Single cell suspensions of lungs harvested from C57BL/6 mice in a standard house dust mite model of asthma were employed to establish a flow cytometric method and compare collagen production in asthmatic and non-asthmatic lungs. Cells found to be CD45$^-$αSMA$^+$, indicative of myofibroblasts, were gated, and median fluorescence intensity of the anti-collagen-I antibody labeling the cells was calculated. Lung myofibroblasts with no, medium, or high levels of collagen-I expression were distinguished. In asthmatic animals, collagen-I levels were increased in both medium and high expressers, and the number of myofibroblasts with high collagen-I content was elevated. Our findings determined that quantification of collagen-I deposition in myofibroblastic lung cells by flow cytometry is feasible in mouse models of asthma and indicative of increased collagen-I expression by asthmatic myofibroblasts.

Keywords

myofibroblast; collagen-I; airway; flow cytometry

Introduction

Tissue fibrosis occurs throughout the body, across multiple organs and organ systems, as a result of both disease and non-disease related damage. When this damage continually affects a tissue, the wound-healing response becomes persistent and can eventually dysregulate [1]. Quantification of collagen deposition in tissue has been a topic of research throughout the past century. Several methods of quantification precede the flow cytometric method

Corresponding author: Kewal Asosingh, Ph.D., asosink@ccf.org, Lerner Research Institute, Cleveland Clinic, Department of Pathobiology, NC22, 9500 Euclid Ave, OH 44195, USA, Phone: + 216-444-0981.

described here, each possessing advantages and disadvantages surrounding their procedures and results, as summarized in Table 1.

The major early method of collagen quantification involved a colorimetric assay used to determine the hydroxyproline content of acid hydrolysates derived from collagen extracts [2]. This method is employed to determine the percent of dry fat-free weight made up by collagen in small quantities of tissues. Hydroxyproline is targeted as a means of quantification as it is present in significant amounts in no other tissue besides collagen and elastin. Collagen has been shown to contain 13.4±0.24 percent hydroxyproline [3]. The hydroxyproline content of elastin, however, is only 1.5 to 2.3 percent, which can easily be adjusted for following data acquisition, allowing for accurate quantification of collagen deposition by this colorimetric assay [2].

Over time, alterations were made to this procedure, some of which aimed to bypass the autoclaving of full tissues required to extract collagen for analysis. Eliminating treatment with urea, which removes tyrosine-containing proteins also extracted by autoclaving, was also targeted. One novel method employs alkali hydrolysis as opposed to acid hydrolysis [4]. Alkali hydrolysis avoids the extended autoclaving required prior to acid hydrolysis, reducing the total duration of collagen quantification, but requires strict adherence to optimized reaction intervals along each step of the protocol. This procedure has also been shown to result in lower yields of hydroxyproline [4].

Independent from the biochemical approach of hydroxyproline analysis, histological methods of collagen deposition quantification have been developed. Masson's Trichrome (MT) employs a staining series which includes xylene, Bouin's solution, hematoxylin, various acidic treatments, and aniline blue in order to stain Paraffin-embedded tissue samples. This process stains collagen (blue), myoplasm (red), and nuclei (brown) [5]. One method of quantifying collagen content following staining is converting micrographs of the MT stained slides into grayscale, and performing an automated count of pixels with a brightness corresponding to the converted blue color of the stained tissue [5,6]. This method is effective for staining both collagen-I and collagen-III, but also includes background staining of fibroblasts and other cells, which brings the sensitivity and specificity of the method into question [6].

Enzyme-linked immunosorbent assay (ELISA) has also been adapted to the detection of collagen deposition. In an early form of this method, collagen-I and collagen-III are isolated by acetic acid extraction and subsequent salt precipitations, while collagen-II is extracted with sodium chloride and purified through chromatography [7]. Each collagen sample is then dissolved in coating buffer and placed in polystyrene microtiter plates used for ELISA. Antibodies are introduced to the antigen, and substrates are added which allow for the absorbance to be recorded by means of a colorimetric assay, which can indicate collagen deposition. ELISA has since been further developed, and centers on the Collagen Type I Carboxy-terminal Peptide (CICP), which is cleaved in the process of collagen biosynthesis [8]. Collagen with uncleaved CICP is termed procollagen and complicates this CICP ELISA method. Procollagen is not fully developed collagen and can obscure the quantification of collagen deposition desired in a study such as ours. A solution to this complication involves

the filtration of the tissue media being studied, which removes any uncleaved procollagen, and allows for the quantification of only true, CICP-cleaved collagen [8]. Therefore, the commercially available CICP ELISA must be used cautiously, in that it requires the filtration of procollagen before accurate quantification of true collagen levels can be achieved.

Asthma is known to present with airway remodeling resulting from subepithelial fibrosis attributed to deposits by myofibroblasts in the extracellular matrix [9,10,11]. In clinical studies, these deposits have been shown to consist mainly of collagens I, III, V, and fibronectin [12,13]. The excess collagen appears throughout the layers of the airway, most notably in the reticular lamina of the subepithelial tissue [12,14].

The aim of the present study was to develop a novel flow cytometric method that can be employed to quantify airway fibrosis; specifically, detecting collagen-I synthesis in the myofibroblast itself rather than waiting for the collagen to be detectable in the extracellular matrix, as is required in biochemical, histological, immunohistochemical, and other current methods.

Methods

Animals and Asthma Model

Female C57BL/6 mice between 8 and 12 weeks old were purchased from Jackson Laboratory. The standard house dust mite model of asthma was used, as described previously [15,16]. All animal experiments were approved by the Cleveland Clinic Institutional Animal Care and Use Committee, protocol #2016-1679.

Lung Single Cell Suspension

Lungs were harvested from C57BL/6 mice (Jackson Laboratory, Bar Harbor, ME) and isolated from surrounding tissue. The lungs were rinsed with PBS and mechanically dispersed and minced with scissors. A quantity of 2.5 mL digestion buffer, comprised of 100 mg/mL Dispase II (Roche Diagnostics, Indianapolis, IN, Cat# 04942078001), 10 mg/mL Collagenase A (Roche Diagnostics, Indianapolis, IN, Cat# 10103578001), 1500 kU/mL DNase I (Sigma-Aldrich, St. Louis, MO, Cat# D5025-150KU), and 0.025M $CaCl_2$ was used per lung for incubation on an orbital shaker at 37°C for 1 hour. The suspension was gently mixed using a pipet and further incubated for 30 minutes before being filtered through a 40μm filter into a 50 mL Falcon tube. The suspension was centrifuged at 900g for 5 minutes using a *Beckman Coulter, Allegra X-12R Centrifuge,* and the supernatant was aspirated. The pellet was resuspended in UV Live/Dead dye (Invitrogen, Waltham, MA, Cat# L23105), according to the manufactures instructions, and incubated in the dark at room temperature for 30 minutes. PBS was added to the suspension, centrifuged at 900g for 5 minutes, and the supernatant was aspirated. Cells were fixed in 4% paraformaldehyde (Polysciences, Warrington, PA, Cat#: 18814-10) in PBS (10 mL 16% PFA diluted in 30 mL PBS) for 10 minutes, followed by an additional washing step used for staining. Fixed cells can also be cryopreserved for antibody staining at a later time point.

Antibody Staining

Fc-receptors were first blocked by pre-incubation of cells for 10 minutes with unconjugated anti-CD16/CD32 antibodies (eBioscience, San Diego, CA, Clone: 93, Cat# 14-0161-85, 1/50 dilution) in 50 μL of 0.1% saponin (Sigma-Aldrich, St. Louis, MO, Cat# S4521) and 1% BSA (Sigma-Aldrich, St. Louis, MO, Cat# A3059-100G) in PBS per tube. After the pre-incubation, 50 μL of a cocktail of the following antibodies were added: anti-CD45-Alexa Fluor 700 (eBioscience, San Diego, CA, Clone: 30-F11, Cat# 56-0451-80, 1/50 dilution), anti-αSMA-FITC (Sigma-Aldrich, St. Louis, MO, Clone: 1A4, Cat# F3777, 1/1600 dilution), and unconjugated anti-collagen-I (Abcam, Cambridge, England, Clone: Polyclonal, Cat# ab34710,1/200 dilution). Antibody cocktails were prepared in 0.1% saponin, 1% BSA buffer containing Fc-block. Following a 30 minute incubation, cells were washed with 500 μL of 0.1% saponin and 1% BSA buffer, centrifuged at 500g for 5 minutes, and aspirated. 50 μL of APC conjugated donkey anti-rabbit (DαR) secondary antibody (Jackson ImmunoResearch Laboratories, West Grove, PA, Clone: Polyclonal, Cat# 711-136-152, 1/100 dilution) was added and cells incubated for 30 minutes. A final wash and centrifugation were performed, and cells were resuspended in 100 μL of FACSFlow (Becton Dickenson, Franklin Lakes, NJ, Cat# 342003). All antibodies were titrated to determine their optimal staining concentration. For the titration of anti-collagen-I, cells were pre-stained with pan-hematopoietic antigen CD45.

All samples were run on a *Becton Dickenson LSRFortessa* flow cytometer. The instrument was set up and standardized using BD Cytometer Setup and Tracking (CS&T) procedures according to manufacturer specifications [17]. 500,000 events per tube were collected and saved as list mode files. Data were analyzed using *FlowJo 10.0.7* software. Student's t-test was used for statistical analysis.

Results

Titration of Anti-collagen-I Antibody Using Lung Single Cell Suspension

Anti-collagen-I antibody, paired with APC conjugated DαR secondary antibody, was titrated using lung single cell suspension pre-stained with pan-hematopoietic antigen CD45. The vast majority of hematopoietic cells are negative for collagen-I, serving as an internal negative control for each anti-collagen-I antibody dilution. Three clusters of cells were observed based on forward and side scatter properties (Figure 1A). Collagen-I expression in each cluster was evaluated in search of the most distinct collagen-I positive subset to determine the optimal dilution of the anti-collagen-I antibody for experiments. Subsets with low/intermediate forward and side scatter (subsets 2 and 3 in Figure 1A) were comprised of a population of CD45 negative cells that bound anti-collagen-I in a similar pattern as the CD45 negative population and were therefore not useful to determine the optimal anti-collagen-I antibody dilution. The subset with high side scatter (subset 1 in Figure 1A) had a population of CD45 negative cells showing clear titration of the anti-collagen-I antibody (Figure 1B). Stain Index was calculated on this subset (Figure 1C) with the equation SI = $(MFI_1 - MFI_2)/2*SD$, where MFl_1=median fluorescence intensity positive population, MFl_2=median fluorescence intensity negative population, and SD=standard deviation negative population. The 1/200 dilution was chosen for experiments.

Expression of Collagen-I in Lung Myofibroblasts in Asthma

Expression of collagen-I in lung myofibroblasts was analyzed in control mice (n=4) and animals with asthma (n=4), for a total sample size of 8 mice. Gating strategy is shown in Figure 2. Time gating was performed on a side scatter/time plot to check for any fluidic disturbances in the flow cell. Doublet events were excluded using a forward scatter-height/forward scatter-area plot, followed by exclusion of cell debris on a forward scatter/side scatter graph. CD45 negative live cells were gated to analyze αSMA positive cells, followed by quantification of collagen-I expression. Background subtracted collagen-I net median fluorescence intensity (MFI) was determined on the CD45$^-$αSMA$^+$ cells. Background fluorescence values were obtained from samples stained in an identical way, but without anti-collagen-I antibody. The collagen-I expression profile (Figure 2F) showed no, medium, and high collagen-I expressing CD45$^-$αSMA$^+$ cells. The percentage, absolute numbers, and MFI of collagen-I expressing cells are summarized in Table 2. There were no differences in percentages or absolute numbers of CD45$^-$αSMA$^+$ cells between control and asthmatic mice. Collagen-I content in medium or high expressers (CD45$^-$αSMA$^+$ collagen$^+$ or CD45$^-$αSMA$^+$ collagen^{++} cells) was significantly higher in the asthma group. Interestingly, control animals had a higher percentage of CD45$^-$αSMA$^+$ collagen$^+$ cells than asthmatic mice. In contrast, both percentage and absolute numbers of CD45$^-$αSMA$^+$ collagen^{++} cells were increased in the asthma group. The findings establish that flow cytometric quantification of collagen-I in myofibroblastic lung cells is feasible in mouse models of asthma and indicates increased collagen-I expression by asthmatic myofibroblasts.

Discussion

Here a flow cytometric method that allows detection of collagen-I content in lung myofibroblasts is described. This novel method included mechanically and enzymatically disaggregated solid tissue in which cells are stained with a viability dye and then fixed prior to permeabilization and antibody staining. There are several advantages to this approach. Sample preparation is a critical step in flow cytometry, specifically for a solid tissue such as the lungs with a high degree of cellular heterogeneity tightly bound together by abundant extracellular matrix. Experiments in mouse models are costly and it is desirable to obtain the maximum amount of high quality data from each experiment with as little variability introduced by technical steps as possible. Processing of lungs from a large group of mice (+10) for flow cytometry can be time consuming. It is challenging to finish endpoint measurements in the live animal, harvest and process the lung tissue into single cell suspension, perform staining for specific markers, and acquire flow cytometric data on the samples within a normal eight to ten hour workday. Often, experiments include multiple groups and are run over several days. The novel method described here may allow high-throughput or batch flow cytometric acquisition of all mice lungs from a specific experiment in a single run. This would be helpful to reduce variability in data due to batch effects and reduce the workload on days of organ harvest. In our experience, the mild fixation with paraformaldehyde prevented disaggregated lung cells from fragmenting during the staining procedure and maintained light scatter properties. Lung cells comprise a very heterogeneous population and processing of unfixed cells resulted in increased cell death and fragmentation of cells. Another advantage of staining with a fixable live/dead dye that is also suitable for

cryopreservation is that it allows easy shipping of frozen samples to other laboratories in collaborative studies. Fluorescent cell barcoding is a powerful technique allowing high-throughput flow cytometric acquisition. Fixed cells can also readily be fluorescently barcoded, reducing the total number of tubes, reagents, and potential artificial variability in the data introduced by staining/acquisition on different days. This cutting edge method allows multiplexing of samples individually stained with different concentrations of a N-hydroxysuccinimide dye in one single tube [18,19,20]. Unmixing of the samples is performed by simple gating of each cluster on a dye datagram during data analysis. Denaturation of proteins due to fixation with formaldehyde may alter antigenicity of proteins and therefore antibody recognition of fixed cells should be tested beforehand for each specific antibody.

Quantification of airway fibrosis is a critical measure in asthma. Most fibrotic disease results from chronic exposure to toxins, irritants, and other persistent challenges [1]. The two major morphologic features of tissues classified as fibrotic include a loss of cellular homeostasis and the accumulation of extracellular matrix, which in turn lead to altered tissue architecture and impaired organ function [21]. This fibrotic mechanism accompanies both the innate and the adaptive immune response to disease and tissue damage, preventing pathogen and microbe entry and spread while also scarring to prevent blood loss and to facilitate regeneration of damaged tissue [1,21]. Although this fibrotic response is a normal physiological mechanism ultimately working to defend an organism and heal damaged tissue, the accompanying effects can have a negative impact on the organism [21].

Airway remodeling associated with subepithelial fibrosis is derived substantially from myofibroblasts [9,10,11]. These myofibroblasts exhibit characteristics of both fibroblasts and myocytes, with secretory and contractile phenotypes, on account of their transformation from fibroblasts following specific signaling pathways [22,23]. Studies of bleomycin-induced pulmonary fibrosis in rats have indicated myofibroblasts as the major, if not sole, contributor to increased lung collagen expression [10].

Airway fibrosis in asthma is detrimental and contributes to disease severity. Upon contraction of airway smooth muscles, the luminal boundary buckles, resulting in a distinct folding pattern of the luminal wall. The thickening of the subepithelial layer results in fewer luminal folds upon buckling, which leads to a greater likelihood of airway obstruction [24]. This increased subepithelial thickness has also been shown to decrease distensibility of the airway, which leads to nonreversible airway obstruction in affected individuals [25]. Elevated subepithelial TGF-β is a prerequisite to collagen accumulation [26]. Airway epithelial cells challenged by airborne allergens and irritants [27,28], along with recruited eosinophils [29,30], both release TGF-β, the main pro-fibrotic cytokine [31]. Clinical studies showed elevation in TGF-β levels and subsequent collagen deposition in the airway within 48 hours of allergen exposure or methacholine-induced bronchoconstriction [32].

TGF-β receptors on the cell surface of fibroblasts signal via Smad-3 to initiate the phenotypic change from fibroblast to myofibroblast [33]. The TGF-β induced upregulation of the cytoskeletal protein α-smooth muscle actin (α-SMA) is a direct characteristic of fibroblast activation and transformation to the myofibroblast phenotype [23,31]. Interleukin-5 (IL-5) also plays a role in this pathway, stimulating the release of TGF-β by eosinophils [34].

Mouse models have demonstrated that the pathway leading to airway fibrosis can be disrupted by inhibition of either IL-5 or Smad-3 genes, which indicates two possible treatment targets for airway fibrosis [33][34][35].

The reticular lamina layer of the subepithelial tissue contains a majority of the excess deposits of collagens I, III, V, and fibronectin observed in the asthmatic, fibrotic airway [12]. The thickening of this reticular lamina, the result of airway remodeling by fibrosis, has been shown to occur to a significantly greater degree in asthmatic patients. One study showed the reticular lamina in non-asthmatic control subjects to be 4–5 μm thick, while asthmatics displayed a reticular lamina thickness between 7 and 23 μm [14]. Other groups have observed at least a doubling in the thickness of this layer, from 5–8 μm in control patients to 10–15 μm in asthmatic individuals [12]. Within the asthmatic population, a positive correlation exists between severity of asthma and degree of subepithelial thickening [36][37]. A few studies have addressed a potential link between airway fibrosis and neutrophilic airway inflammation. Endobronchial biopsies in patients with either severe, moderate, or non-asthmatic phenotypes found a positive correlation between eosinophil levels and airway fibrosis in the subepithelial layer. A subset of patients with severe neutrophilic asthma, however, did not have abnormal amounts of subepithelial fibrosis [38]. Generally, neutrophils are regarded to play a lesser role, if any, in airway fibrosis in contrast to eosinophils [39].

Our novel flow cytometric method enables objective quantification of collagen while excluding nonspecific interference such as cell debris, dead cells, doublets or aggregated cells, and hematopoietic cells, which may be present in the tissue samples being studied. Flow cytometry of CD45$^-$αSMA$^+$ cells, indicative of myofibroblasts [40][41], enables a snapshot of current collagen-I biosynthesis and deposition and excludes collagen-I which has been present in the tissue for an unknown period of time. However, this entails that cumulative collagen deposition in the extracellular space is not detected. Also noteworthy is that the use of a directly conjugated anti-collagen-I-APC antibody, rather than pairing with a secondary APC conjugated antibody, as employed here, would allow for absolute quantification and results to be reported in molecules of equivalent soluble fluorescence (MESF). Grouping of the lung myofibroblasts into medium and high collagen-I expressing cells provided additional insight into the biology of these cells in asthma. The data suggested that while under physiological conditions the majority of the myofibroblasts expressed medium levels of collagen-I. This pool of medium expressers is decreased in asthma. The doubling of the frequency and absolute numbers of high collagen-I expressers may suggest a shift of medium expressers into high expressers during asthma. The novel technique described here will be useful to evaluate therapeutic effects on extracellular remodeling much earlier by quantification of collagen synthesis in the myofibroblast itself rather than having to quantify changes in collagen deposition in the extracellular matrix during later stages of the disease.

Acknowledgments

References

1. Duffield JS, Lupher M, Thannickal VJ, Wynn TA. Host responses in tissue repair and fibrosis. Annu Rev Pathol. 2013; 8:241–76. [PubMed: 23092186]

2. Neuman RE, Logan MA. The determination of collagen and elastin in tissues. J Biol Chem. 1950; 186:549–56. [PubMed: 14794650]

3. Neuman RE, Logan MA. The determination of hydroxyproline. J Biol Chem. 1950; 184:299–306. [PubMed: 15421999]

4. Hofman K, Hall B, Cleaver H, Marshall S. High-throughput quantification of hydroxyproline for determination of collagen. Anal Biochem. 2011; 417:289–91. [PubMed: 21741948]

5. Yan J, Thomson JK, Wu X, Zhao W, Pollard AE, Ai X. Novel methods of automated quantification of gap junction distribution and interstitial collagen quantity from animal and human atrial tissue sections. PLoS One. 2014; 9:e104357. [PubMed: 25105669]

6. Calvi EN, Nahas FX, Barbosa MV, Calil JA, Ihara SS, Juliano Y, Ferreira LM. Collagen fibers in the rectus abdominis muscle of cadavers of different age. Hernia. 2014; 18:527–33. [PubMed: 24415040]

7. Gosslau B, Barrach HJ. Enzyme-linked immunosorbent microassay for quantification of specific antibodies to collagen type I, II, III. J Immunol Methods. 1979; 29:71–7. [PubMed: 489989]

8. Kopanska KS, Powell JJ, Jugdaohsingh R, Bruggraber SF. Filtration of dermal fibroblast-conditioned culture media is required for the reliable quantitation of cleaved carboxy-terminal peptide of collagen type I (CICP) by ELISA. Arch Dermatol Res. 2013; 305:741–5. [PubMed: 23732861]

9. Redington AE. Fibrosis and airway remodelling. Clin Exp Allergy. 2000; 30(Suppl 1):42–5. [PubMed: 10849474]

10. Zhang K, Rekhter MD, Gordon D, Phan SH. Myofibroblasts and their role in lung collagen gene expression during pulmonary fibrosis. A combined immunohistochemical and in situ hybridization study. Am J Pathol. 1994; 145:114–25. [PubMed: 7518191]

11. Brewster CE, Howarth PH, Djukanovic R, Wilson J, Holgate ST, Roche WR. Myofibroblasts and subepithelial fibrosis in bronchial asthma. Am J Respir Cell Mol Biol. 1990; 3:507–11. [PubMed: 2223105]

12. Roche WR, Beasley R, Williams JH, Holgate ST. Subepithelial fibrosis in the bronchi of asthmatics. Lancet. 1989; 1:520–4. [PubMed: 2466184]

13. Homer RJ, Elias JA. Airway remodeling in asthma: therapeutic implications of mechanisms. Physiology (Bethesda). 2005; 20:28–35. [PubMed: 15653837]

14. Homer RJ, Elias JA. Consequences of long-term inflammation. Airway remodeling. Clin Chest Med. 2000; 21:331–43. ix. [PubMed: 10907592]

15. Plantinga M, Guilliams M, Vanheerswynghels M, Deswarte K, Branco-Madeira F, Toussaint W, Vanhoutte L, Neyt K, Killeen N, Malissen B, Hammad H, Lambrecht BN. Conventional and monocyte-derived CD11b(+) dendritic cells initiate and maintain T helper 2 cell-mediated immunity to house dust mite allergen. Immunity. 2013; 38:322–35. [PubMed: 23352232]

16. Hammad H, Plantinga M, Deswarte K, Pouliot P, Willart MA, Kool M, Muskens F, Lambrecht BN. Inflammatory dendritic cells--not basophils--are necessary and sufficient for induction of Th2 immunity to inhaled house dust mite allergen. J Exp Med. 2010; 207:2097–111. [PubMed: 20819925]

17. Meinelt E, Reunanen M, Edinger M, Jaimes M, Stall A, Sasaki D, Trotter J. Standardizing Application Setup Across Multiple Flow Cytometers Using BD FACSDiva™ Version 6 Software. BD Biosciences Technical Bulletin. 2012

18. Giudice V, Feng X, Kajigaya S, Young NS, Biancotto A. Optimization and standardization of fluorescent cell barcoding for multiplexed flow cytometric phenotyping. Cytometry A. 2017; 91:694–703. [PubMed: 28692789]

19. Krutzik PO, Clutter MR, Trejo A, Nolan GP. Fluorescent cell barcoding for multiplex flow cytometry. Curr Protoc Cytom. 2011; Chapter 6(Unit 6):31.

20. Krutzik PO, Nolan GP. Fluorescent cell barcoding in flow cytometry allows high-throughput drug screening and signaling profiling. Nat Methods. 2006; 3:361–8. [PubMed: 16628206]

21. Thannickal VJ, Zhou Y, Gaggar A, Duncan SR. Fibrosis: ultimate and proximate causes. J Clin Invest. 2014; 124:4673–7. [PubMed: 25365073]

22. Tagaya E, Tamaoki J. Mechanisms of airway remodeling in asthma. Allergol Int. 2007; 56:331–40. [PubMed: 17965576]

23. Royce SG, Cheng V, Samuel CS, Tang ML. The regulation of fibrosis in airway remodeling in asthma. Mol Cell Endocrinol. 2012; 351:167–75. [PubMed: 22266540]

24. Wiggs BR, Hrousis CA, Drazen JM, Kamm RD. On the mechanism of mucosal folding in normal and asthmatic airways. J Appl Physiol (1985). 1997; 83:1814–21. [PubMed: 9390950]

25. Shifren A, Witt C, Christie C, Castro M. Mechanisms of remodeling in asthmatic airways. J Allergy (Cairo). 2012; 2012:316049. [PubMed: 22315625]

26. Kumar RK, Herbert C, Kasper M. Reversibility of airway inflammation and remodelling following cessation of antigenic challenge in a model of chronic asthma. Clin Exp Allergy. 2004; 34:1796–802. [PubMed: 15544607]

27. Redington AE, Madden J, Frew AJ, Djukanovic R, Roche WR, Holgate ST, Howarth PH. Transforming growth factor-beta 1 in asthma. Measurement in bronchoalveolar lavage fluid. Am J Respir Crit Care Med. 1997; 156:642–7. [PubMed: 9279252]

28. Kumar RK, Herbert C, Foster PS. Expression of growth factors by airway epithelial cells in a model of chronic asthma: regulation and relationship to subepithelial fibrosis. Clin Exp Allergy. 2004; 34:567–75. [PubMed: 15080809]

29. Kariyawasam HH, Robinson DS. The role of eosinophils in airway tissue remodelling in asthma. Curr Opin Immunol. 2007; 19:681–6. [PubMed: 17949963]

30. Holgate ST. Pathogenesis of asthma. Clin Exp Allergy. 2008; 38:872–97. [PubMed: 18498538]

31. Lin CH, Shen ML, Kao ST, Wu DC. The effect of sesamin on airway fibrosis in vitro and in vivo. Int Immunopharmacol. 2014; 22:141–50. [PubMed: 24978608]

32. Grainge CL, Lau LC, Ward JA, Dulay V, Lahiff G, Wilson S, Holgate S, Davies DE, Howarth PH. Effect of bronchoconstriction on airway remodeling in asthma. N Engl J Med. 2011; 364:2006–15. [PubMed: 21612469]

33. Cho JY, Miller M, Baek KJ, Han JW, Nayar J, Lee SY, McElwain K, McElwain S, Friedman S, Broide DH. Inhibition of airway remodeling in IL-5-deficient mice. J Clin Invest. 2004; 113:551–60. [PubMed: 14966564]

34. Le AV, Cho JY, Miller M, McElwain S, Golgotiu K, Broide DH. Inhibition of allergen-induced airway remodeling in Smad 3-deficient mice. J Immunol. 2007; 178:7310–6. [PubMed: 17513781]

35. Flood-Page P, Menzies-Gow A, Phipps S, Ying S, Wangoo A, Ludwig MS, Barnes N, Robinson D, Kay AB. Anti-IL-5 treatment reduces deposition of ECM proteins in the bronchial subepithelial basement membrane of mild atopic asthmatics. J Clin Invest. 2003; 112:1029–36. [PubMed: 14523040]

36. Chetta A, Foresi A, Del Donno M, Bertorelli G, Pesci A, Olivieri D. Airways remodeling is a distinctive feature of asthma and is related to severity of disease. Chest. 1997; 111:852–7. [PubMed: 9106559]

37. Djukanovic R, Lai CK, Wilson JW, Britten KM, Wilson SJ, Roche WR, Howarth PH, Holgate ST. Bronchial mucosal manifestations of atopy: a comparison of markers of inflammation between atopic asthmatics, atopic nonasthmatics and healthy controls. Eur Respir J. 1992; 5:538–44. [PubMed: 1612155]

38. Wenzel SE, Schwartz LB, Langmack EL, Halliday JL, Trudeau JB, Gibbs RL, Chu HW. Evidence that severe asthma can be divided pathologically into two inflammatory subtypes with distinct physiologic and clinical characteristics. Am J Respir Crit Care Med. 1999; 160:1001–8. [PubMed: 10471631]

39. Fahy JV. Eosinophilic and neutrophilic inflammation in asthma: insights from clinical studies. Proc Am Thorac Soc. 2009; 6:256–9. [PubMed: 19387026]

40. Akamatsu T, Arai Y, Kosugi I, Kawasaki H, Meguro S, Sakao M, Shibata K, Suda T, Chida K, Iwashita T. Direct isolation of myofibroblasts and fibroblasts from bleomycin-injured lungs reveals their functional similarities and differences. Fibrogenesis Tissue Repair. 2013; 6:15. [PubMed: 23927729]

41. Fujita J, Mori M, Kawada H, Ieda Y, Tsuma M, Matsuzaki Y, Kawaguchi H, Yagi T, Yuasa S, Endo J, Hotta T, Ogawa S, Okano H, Yozu R, Ando K, Fukuda K. Administration of granulocyte colony-stimulating factor after myocardial infarction enhances the recruitment of hematopoietic stem cell-derived myofibroblasts and contributes to cardiac repair. Stem Cells. 2007; 25:2750–9. [PubMed: 17690181]
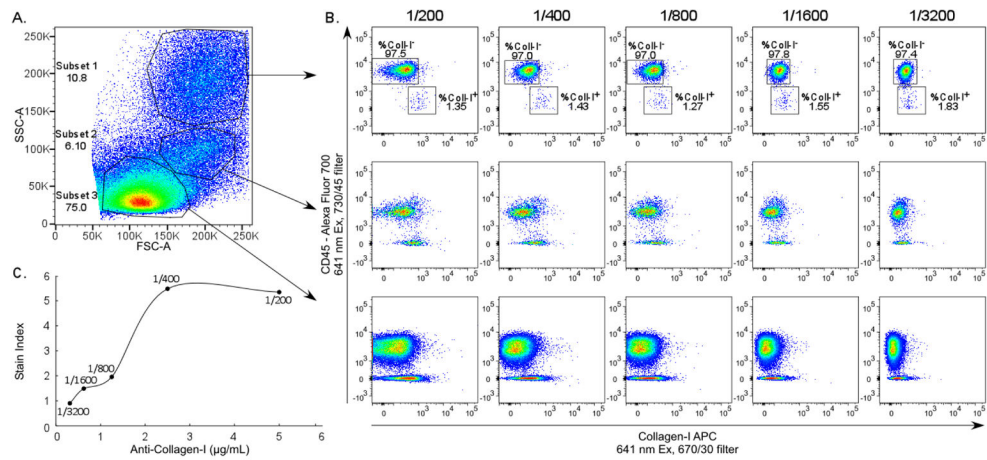
Figure 1.
Titration of anti-collagen-I Antibody Using Lung Single Cell Suspension. Lung single cell suspensions were used to determine the optimal dilution of anti-collagen-I antibody. (**A**) Three subsets of cells were distinguished based on forward and side scatter. (**B**) Analysis of anti-collagen-I binding in each subset. Ratios indicate antibody dilution. (**C**) Stain Index of anti-collagen-I on Subset 1. Lines between data points were connected using the "Smoothed Line" feature in Microsoft Excel 2013.
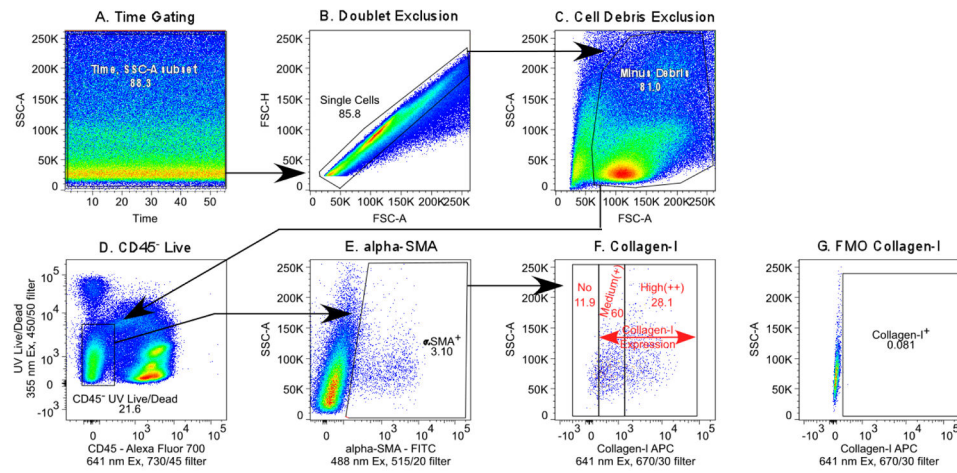
Figure 2.
Gating of collagen-I positive lung myofibroblasts. (**A**) Time gating. (**B**) Exclusion of doublet events. (**C**) Exclusion of debris. (**D**) Exclusion of hematopoietic and dead cells. (**E**) Selection of αSMA positive cells. (**F**) Gating of collagen-I positive cells and (**G**) collagen-I gating control.

Table 1

Overview of Other Collagen Quantification Methods

COLLAGEN QUANTIFICATION METHOD	HOW IT MEASURES	WHAT IT MEASURES	ADVANTAGES	DISADVANTAGES
Hydroxyproline – Acid Hydrolysis	Colorimetric assay to determine content of hydroxyproline in acid hydrolysates	Hydroxyproline content of tissue, an amino acid derived mainly from collagen	-Higher hydroxyproline yields than alkali hydrolysis -Yields simple percentage of collagen in dry tissue	-Must adjust for hydroxyproline contributed by elastin - Long duration procedure including overnight autoclaving of tissue -Small quantities of tissue processed at a time leads to sampling error
Hydroxyproline – Alkali Hydrolysis	Colorimetric assay to determine content of hydroxyproline in alkali hydrolysates	Hydroxyproline content of tissue, an amino acid derived mainly from collagen	-Autoclaving not required -Shorter overall duration -Treatment with urea not needed	-Very specific, strict incubation and reaction steps in procedure -Lower hydroxyproline yields than acid hydrolysis -Small quantities of tissue processed at a time leads to sampling error
Trichrome	Immunohistochemical staining of collagen fibers with aniline blue dye	Overall percentage of stained collagen pixels in micrographs of whole tissue	-Visual, histological approach -Does not depend on biochemical reaction conditions	-Includes background staining from myofibroblasts and other cells -Subject to sampling error
CICP ELISA	Colorimetric assay to determine content of antibody labeled CICP	Collagen type I carboxy-terminal peptide, cleaved in process of collagen biosynthesis	-Minimal tissue isolation and preparation required	-Must be filtered to eliminate procollagen and allow quantification of only cleaved CICP -Small quantities of tissue processed at a time leads to sampling error

Table 2

Collagen-I and Lung Myofibroblast in C57BL/6 Mice

MEASURE	CONTROL (n=4)	ASTHMA (n=4)	p-VALUE
% CD45$^-$αSMA$^+$ cells	2.8 ± 0.2	2.6 ± 0.08	NS
# CD45$^-$αSMA$^+$ cells (10^3)	304 ± 17	326 ± 8	NS
Collagen-I content in collagen$^+$ cells	398 ± 53	751 ± 51	0.002
Collagen-I content in collagen^{++} cells	3004 ± 29	3224 ± 32	0.002
% CD45$^-$αSMA$^+$collagen$^+$ cells	2.4 ± 0.1	1.8 ± 0.04	0.007
% CD45$^-$αSMA$^+$collagen^{++} cells	0.49 ± 0.4	0.87 ± 0.05	0.0008
# CD45$^-$αSMA$^+$collagen$^+$ cells (10^3)	254 ± 13	219 ± 3.6	NS
# CD45$^-$αSMA$^+$collagen^{++} cells (10^3)	53 ± 4	108 ± 6	0.002

Collagen-I content = median collagen-I fluorescence intensity minus median background fluorescence intensity of tubes with omitted collagen-I primary antibody.